

KIF5C, a kinesin motor involved in apical trafficking of MDCK cells

Ksenia Astanina · Ralf Jacob

Received: 7 September 2009 / Revised: 22 December 2009 / Accepted: 28 December 2009 / Published online: 22 January 2010
© Birkhäuser Verlag, Basel/Switzerland 2010

Abstract Polarized traffic in epithelial cells depends on well-organized pathways that direct secretory cargo to the apical or basolateral plasma membrane. In MDCK cells, apical trafficking can be further divided into a lipid raft-dependent and a raft-independent route, which separate biosynthetic cargo in a post-Golgi endosomal compartment. We have now identified KIF5C as a kinesin motor for apical trafficking of both raft-associated sucrase isomaltase and raft-independent neurotrophin receptor. KIF5C was identified by mass spectrometry in vesicle enriched fractions and on immunisolated post-Golgi vesicles carrying apical cargo. The amount of vesicle-associated KIF5C was highest on material isolated directly after trans-Golgi network release and declined thereafter. Altogether, our data suggest that KIF5C is involved in the passage of apical cargo molecules to a post-Golgi endosomal compartment, where further segregation into distinct vesicle populations proceeds.

Keywords Kinesin · Apical trafficking · KIF5 · Vesicle movement · MDCK

Introduction

Establishment and maintenance of an intact epithelium is critical for tissue integrity. For this reason the plasma membrane of epithelial cells is divided into two separate membrane compartments, the apical and the basolateral domain. Both domains are composed of different proteins and lipids [1] and are separated by tight junctional complexes. For example, the apical plasma membrane of intestinal enterocytes is enriched with intestinal hydrolases, while E-cadherin is exclusively restricted to the basolateral domain [2]. This polarity is maintained by intracellular machinery that directs newly synthesized material to the correct target membrane [3].

The epithelial trafficking machinery has to ensure that newly synthesized surface proteins move along the secretory pathway to the trans-Golgi network (TGN), where they are sorted into apical and basolateral carriers [4]. Apical post-Golgi vesicles are composed of distinct vesicular components and can take various routes to the cell surface [5, 6]. Some of them depend on the integrity of sphingolipid/cholesterol-enriched membrane microdomains named “lipid rafts”; others use separate transport platforms. Typical marker proteins for lipid raft-dependent apical pathways are sucrase isomaltase (SI) [7], influenza virus haemagglutinin (HA) [8], gp135 [9] and glycosyl-phosphatidylinositol-anchored proteins [10]. For the raft-independent pathway transmembrane proteins such as the neurotrophin receptor (p75) [11], gp114 [12, 13], endolyn [14] and lactase-phlorizin hydrolase [15] are commonly studied.

We have previously found that both raft-associated and raft-independent apical transport pathways depend on the integrity of microtubules, whereas actin microfilaments are mainly required for cell surface delivery of raft-

Electronic supplementary material The online version of this article (doi:10.1007/s00018-009-0253-6) contains supplementary material, which is available to authorized users.

K. Astanina · R. Jacob (✉)
Department of Cell Biology and Cell Pathology,
Philipps University of Marburg, Robert-Koch-Str. 6,
35033 Marburg, Germany
e-mail: jacob@staff.uni-marburg.de

associated SI [5]. Consequently, the delivery of proteins to the apical surface in general depends on microtubular motors such as dynein and kinesin [16]. In view of the fact that epithelial cells extensively remodel their cytoarchitecture after the formation of cell–cell contacts [17], the question arises as to whether plus or minus end-directed traffic or even both are involved in apical protein delivery. Evidence for a role of kinesin as well as dynein in apical delivery of HA came from immunodepletion studies with MDCK cells [18]. Minus end-directed kinesin KIFC3 was then identified in apical trafficking of raft-associated HA and annexin 13b [19]. On the other hand, the plus end-directed motor KIF5B, a member of the kinesin-1 group, is involved in raft-independent apical delivery of p75 in MDCK cells [20]. This particular role of KIF5B is restricted to polarized cells only. In summary, even with a restriction to MDCK cells as model system for polarized trafficking, distinct motors have been published that move along microtubules in opposite directions and carry separate cargo molecules. A general motor implicated in raft-dependent as well as raft-independent pathways has not been identified yet. Therefore, a search for such a motor could not only help to understand the regulation of apical traffic, but also to clarify the points of intersection between these pathways.

In this study, we identified the kinesin-1 group member, KIF5C, as a motor protein for apical trafficking of both, raft-associated SI and raft-independent p75. Biochemical as well as fluorescence microscopic analysis revealed that KIF5C is present on SI- and p75-containing vesicles at early time points after TGN exit. The functional relevance of KIF5C in apical delivery of both transmembrane proteins was demonstrated by depletion of the motor mediated by small interfering RNA (siRNA). Furthermore, confocal data showed the intracellular accumulation of transported material near the apical cell pole of KIF5C-depleted MDCK cells. We could not detect any direct interaction between KIF5C and SI or p75, which suggests that the motor and cargo molecules are indirectly connected. To our knowledge, this is the first example of a motor protein for raft-associated and raft-independent cargo in apical protein transport from the Golgi to the cell surface.

Materials and methods

Cell culture, biosynthetic labelling of cells and immunoprecipitation

MDCK cells were cultured at 37°C in an atmosphere containing 5% CO₂ in minimum essential medium (PAA, Pasching Austria) containing 10% fetal calf serum. Plasmid and siRNA transfection of MDCK cells was performed

with Lipofectamine 2000 (Invitrogen) according to the manufacturer's instructions. Biosynthetic labelling of MDCK_{p75} or MDCK_{SI} cells, accumulation of newly synthesized material in the TGN at 20°C and surface immunoprecipitation were performed essentially as described previously [21]. Images generated on a phosphorimager were analysed using QUANTITY ONE software (BioRad).

Vesicle preparation and precipitation

For the enrichment of post-TGN vesicles, the cells were incubated for 4 h at 20°C to accumulate newly synthesized material in the TGN, followed by TGN release at 37°C for various times. Polarized MDCK_{p75-GFP}, MDCK_{SI-YFP}, or MDCK cells were scraped with a cell scraper in 1.5 ml PMEE buffer plus 250 mM sucrose (35 mM PIPES, pH 7.4, adjusted with NaOH; 5 mM MgCl₂; 1 mM EGTA; 0.5 mM EDTA; 4 mM DTT; sucrose) and homogenized by 20 passages through 26-gauge needle. The homogenates were then centrifuged essentially as described previously [22]. The TGN-38-positive fractions 8, 9 and 10 were used for immunoprecipitation with mAb anti-GFP (Clontech) or pAb anti-KIF5C (Acris Antibodies). The samples were precleared for 1 h at 4°C with PAS (protein-A Sepharose). The PAS was then pelleted and the supernatant was incubated for 1 h with the antibody. PAS beads were added for overnight precipitation. Antigen–antibody complexes were pelleted by centrifugation at 2000×g, and the samples were washed six times with PMEE plus 250 mM sucrose buffer prior to SDS-PAGE analysis.

Motility and binding assay

Rhodamine-labelled and nonlabelled tubulin from bovine brain (Cytoskeleton, Denver, CO) was polymerized according to the manufacturer's instructions. The microtubules were stabilized with Taxol (paclitaxel; Cytoskeleton) and were kept at room temperature for 1–2 days. Vesicle-enriched fractions were used directly for the assay or snap-frozen in liquid nitrogen and stored at –80°C.

The assay itself was adapted from that described by Murray et al. [23] and analysed in a thermally controlled chamber (37°C) on a Leica DMI 6000 fluorescent microscope. Binding assays were adapted from that described by Blocker et al. [24]. For each experimental set at least three independent experiments were analyzed.

Immunofluorescence and confocal fluorescence microscopy

Cells were fixed and prepared for immunofluorescence analysis as described previously [22]. Confocal images of

living cells were acquired on a Leica TCS SP2 AOBS microscope using a $\times 40$ oil plan apochromat lens (Leica Microsystems). For immunostaining, the secondary antibodies anti-mouse Alexa Fluor546, anti-rabbit Alexa Fluor488 and anti-goat Alexa Fluor488 were purchased from Molecular Probes. Data evaluation and colocalization analysis was performed with region of interest detection of the Leica software in combination with the Velocity imaging software package (Improvision).

Immunochemical reagents and immunoblotting

The samples were separated by SDS-PAGE using the Hoefer-Mini-VE system (Amersham Pharmacia Biotech) and transferred to nitrocellulose membranes. Membranes were blocked for 1 h in 5% skimmed milk powder in PBS.

Monoclonal antibodies KHC (kinesin heavy chain) antibody was purchased from US Bio, H1 from Chemicon, H2 from Abcam, anti-GFP (JL-8) from Clontech, anti-GAPDH from Stressgen, anti-dynein intermediate chain from Novus Biologicals, anti-E-cadherin from BD Biosciences. The monoclonal anti-SI antibodies were generously provided by H.P. Hauri (Biozentrum Basel, Switzerland). The monoclonal anti-p75 (ME20.4) antibody was generously provided by A. Le Bivic (Faculté des Sciences de Luminy, Marseille, France).

Polyclonal antibodies Anti-KIF5A antibody was purchased from Abcam, anti-KIF5B antibody from Everest Biotech, anti-KIF5C antibody from Acris Antibodies. The specificities of anti-kinesin antibodies used in this study are presented in Table 1. Rabbit polyclonal antibodies directed against galectin-3 were kindly provided by H.P. Elsaesser (University of Marburg, Germany). Antibody incubations were performed overnight at 4°C. Detection was performed with horseradish peroxidase-conjugated secondary antibodies which were visualized by enhanced chemiluminescence (Signal Plus; Pierce) and an Intas Gel Imager charge-coupled device camera.

RNA interference

MDCK cells were seeded on six-well filters in 3 ml of growth medium. On day 2 and day 3, confluent cells were transfected with 100 pmol of each siRNA duplex in 1.5 ml MEM and 10 μ l Lipofectamine 2000. After 6 h of incubation, the medium was changed to normal growth medium. The cells were analysed 5 days after seeding. For RNA-mediated interference (RNAi) experiments, KIF5B and KIF5C were specifically depleted with the following duplexes:

Table 1 Isotype-specific and nonspecific antibodies directed against KIF5 kinesins

Antibody	Immunogen, epitope	Specificity	Applications	Host and clonality	Company	References
H1	Bovine brain kinesin, N-terminus	KIF5A ^a , KIF5C	Western blot	Mouse, monoclonal	Chemicon International	[29, 37]
H2	Bovine brain kinesin, N-terminus	KIF5A, KIF5B, KIF5C	Immunoprecipitation	Mouse, monoclonal	Abcam	[29, 37]
KHC	Bovine brain kinesin, N-terminus	KIF5A, KIF5B, KIF5C	Western blot	Mouse, monoclonal	US Biological	
KIF5C	Synthetic peptide corresponding to amino acid residues 938–957 from human kinesin 5C. Amino acid sequence: C A(938) VHAIRGGSSNSTHYQK (957)	KIF5C	Immunoprecipitation, immunofluorescence	Rabbit, polyclonal	Acris Antibodies	See Fig. 3a
KIF5B	Peptide with sequence C-QPVAVRGGGKQV, from the C-terminus of the KIF5B protein sequence according to NP_004512.1	KIF5B	Immunoprecipitation, Western blot	Goat, polyclonal	Everest Biotech	See Fig. 3a

^a H1 antibodies have very low affinities for canine KIF5A as depicted in Fig. 2e

For KIF5B: 5'-GAGCAAGUGUAUAAUGACUUU-3'/3'-UUCUCGUUCACAUAUACUGA-5', 5'-AAGCUGAGUGGAAAACUUUUU-3'/3'-UUUUCGACUCACCUUUUGAAA-5', 5'-GGAGUAUGAAUUGCUUAGUU-3'/3'-UUCCUCAUACUUAACGAAUCA-5'

For KIF5C: 5'-UGCAGCAUCAAGGUGAUGUUU-3'/3'-UUACGUCGUAGUCCACUACA-5', 5'-AACCUGAGUUUCACAUCAUU-3'/3'-UUUUGGAUCUCAAGUGUAGU-5', 5'-ACAAGACUCUGAAGAAUGUU-3'/3'-UUUGUUCUGAGACUUCUACA-5'

As a control, luciferase siRNA was used (5'-CGUACGCGGAAUACUUCGATT-3'/5'-UCGAAGUAUUCGCGUACGTT-3').

Proteomic analysis

Electrophoretically separated proteins were excised from Coomassie-stained (Roti-Blue kit, Carl Roth) gels and processed for mass spectrometry in MALDI-TOF mode using a Voyager DE STR instrument (PerSeptive Biosystems, Framingham, MA) or an Ultraflex Instrument (Brucker, Germany) in the group of Dr. Lingelbach (SFB 593, Marburg, Germany). For protein identification, MALDI spectra were explored by database searches with the computer software PROFOUND (<http://prowl.rockefeller.edu/prowl-cgi/profound.exe>) and MASCOT (www.matrixscience.com).

Results

Evidence for tubulin-dependent motors on purified p75-containing post-Golgi vesicles

To study the presence of tubulin motors on apical post-Golgi vesicles, MDCK_{p75-GFP} cells stably expressing the raft-independent apical glycoprotein p75 were incubated for 5 days after confluency for full polarization. Apical transport of newly synthesized material was blocked in the TGN by incubation for 4 h at 20°C followed by a TGN release at 37°C for 10 min. The cells were homogenized and apical post-Golgi vesicles were isolated by sucrose density centrifugation. First, binding of these isolated vesicles was characterized. Purified vesicles were incubated with microtubules in perfusion chambers and unbound material was washed out. Under these conditions about 25–30% of the vesicles remained microtubule-associated (Fig. 1a). The efficiency of binding could be significantly reduced by preheating the vesicles to 80°C for 10 min or by trypsin treatment at 37°C for 15 min before placing in the perfusion chamber with immobilized microtubules. Both treatments

affected the integrity of vesicle-associated polypeptides and thus suggests that purified post-Golgi p75-GFP vesicles bind in vitro to microtubules in a protein-dependent manner.

To determine whether tubulin-dependent motors are involved in this binding capacity, we then performed in vitro motility assays by adding 2.5 mM ATP to microtubule-bound vesicles at 37°C. Images recorded immediately after addition of ATP are indicated in Fig. 1b. Under these conditions some of the microtubule-bound vesicles started to move along the microtubular tracks. In some cases vesicles detached from microtubules and stopped moving, and others attached to microtubules and started moving. Unidirectional (processive) and bidirectional (diffusive) vesicular movements along microtubules are illustrated as kymograms in Fig. 1c. Velocity measurements of 53 vesicles from two independent experiments revealed an average diffusive vesicle speed of about 0.08 μm/s including uni- and bidirectional movements, while unidirectional movements displayed an average velocity of about 0.28 μm/s. Consequently, our observations indicate that purified apical post-Golgi vesicles still carry tubulin-dependent motor proteins and can thus be utilized for their biochemical characterization.

Vesicle-enriched fractions of p75-GFP preparations contain KIF5C

Since bidirectional movement of p75-carrying vesicles along microtubules could be due to the presence of plus or minus end-directed vesicle-associated motor proteins, we decided to analyse immunisolated vesicles with anti-kinesin heavy chain (anti-KHC) and anti-dynein antibodies. As depicted in Fig. 2a, these p75-containing vesicles carried KHC, but no dynein. The kinesin isoforms present on p75-carrying post-Golgi vesicles were then identified and previously characterized vesicle-enriched fractions were subjected to a proteomic analysis [5, 22]. Again, post-Golgi vesicles were harvested 10 min after TGN exit by sucrose density centrifugation. Since it had previously been published that KIF5B, a member of the kinesin-1 group, is required for apical transport of p75 in polarized MDCK cells [20], the question arose as to whether purified vesicles contain additional kinesin-1 variants. Polypeptides were precipitated from vesicle-enriched fractions with anti-kinesin-1 heavy chain H2 antibodies and separated by SDS-PAGE. As depicted in Fig. 2b, several bands appeared in Coomassie blue-stained gels. Immunoblots with KHC antibodies then stained the immunoglobulin heavy chain at about 50 kDa with a band at about 120 kDa. This band was isolated, analysed by mass spectrometry and was identified as KIF5C. For verification, this experiment was performed three times with a significant MASCOT score in the range of 120 for KIF5C. Therefore it

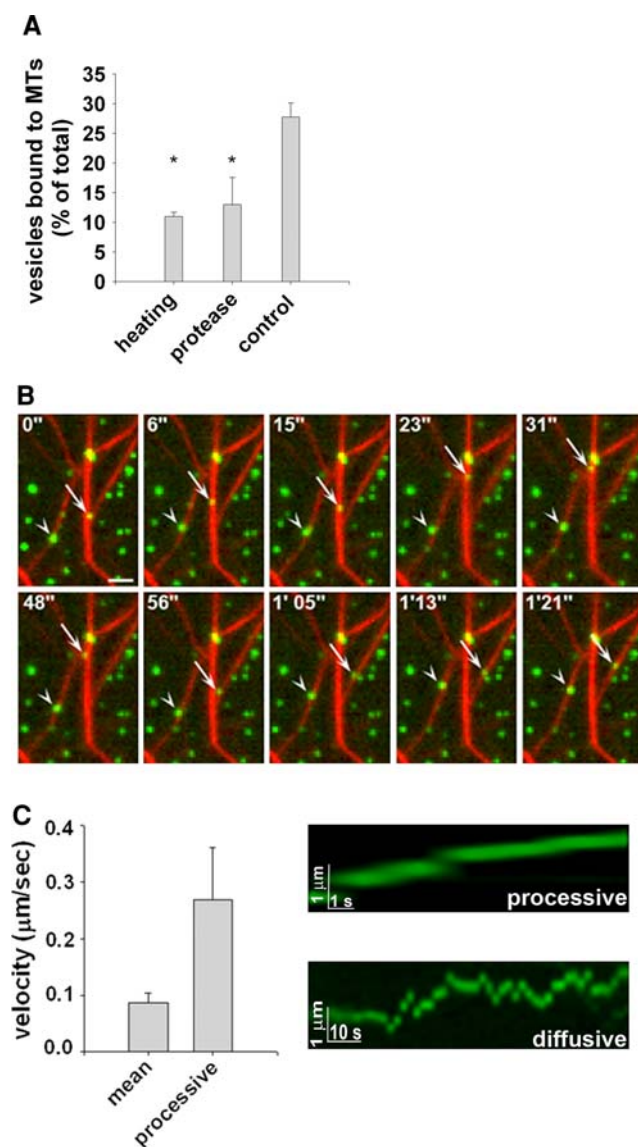


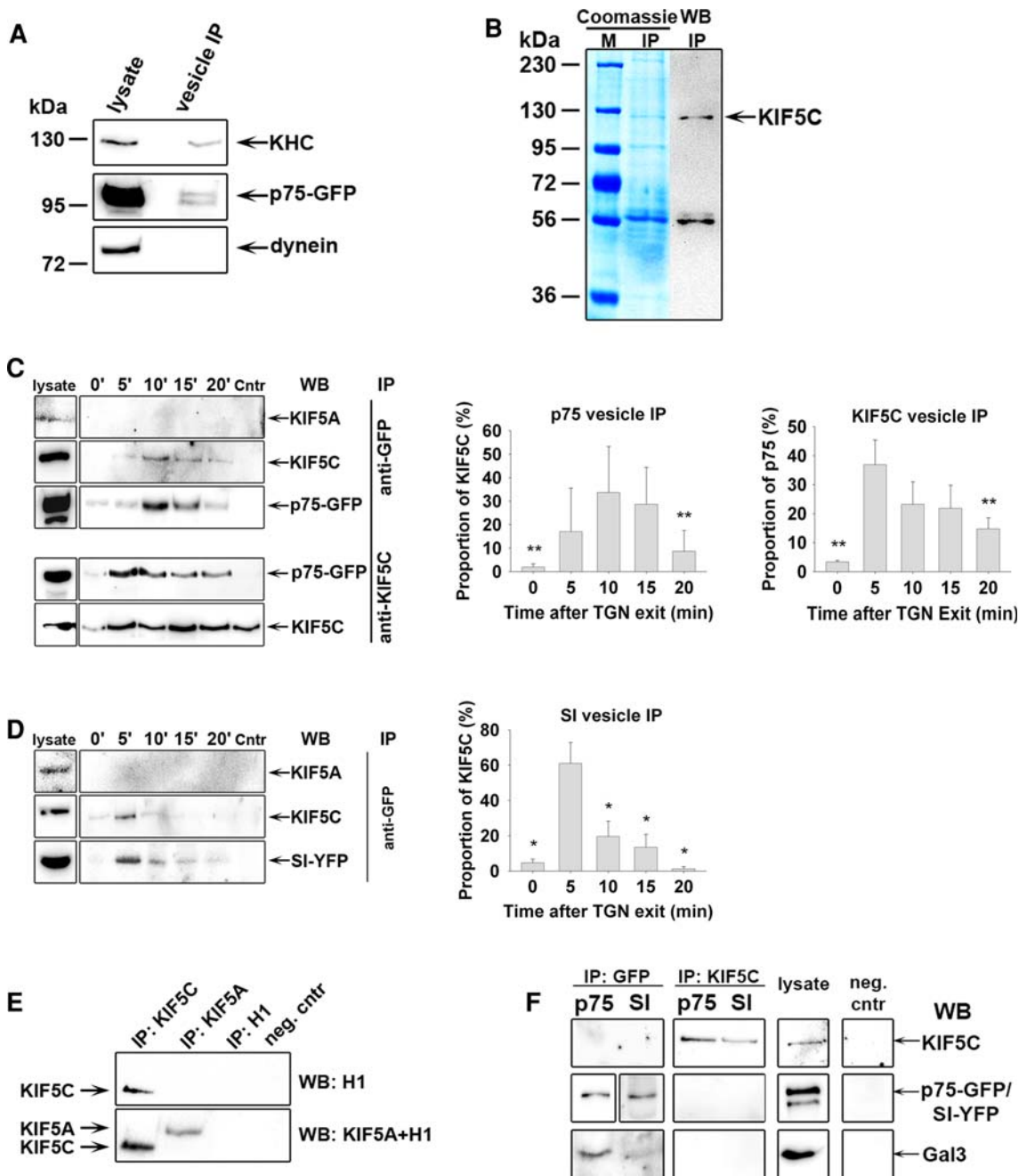
Fig. 1 In vitro motility and binding assay of purified p75-GFP-carrying vesicles. Purified p75-GFP-containing vesicles moved in vitro on rhodamine-labelled microtubules in an ATP-dependent manner. **a** Isolated vesicles were heated or subjected to protease digestion and the efficiency of vesicle binding to microtubules was compared to that in the control experiment. Asterisks denote statistically significant differences in the number of vesicles bound to microtubules using paired Student's *t* tests; * $p < 0.01$; bars standard error. **b** Selected frames from a live cell time-lapse. Moving vesicles are indicated by arrows and arrowheads. The movement is bidirectional, with a switch of microtubular tracks. The time is indicated in minutes (') and seconds ("). Scale bar 1 μm . **c** The velocity of p75-GFP vesicles was measured in three independent experiments. The mean velocity (*mean*) was the mean velocity of both types of movement: unidirectional (*processive*) and bidirectional (*diffusive*) ($n=53$). The velocity of only unidirectional (*processive*) movement was also measured ($n=16$). Example kymographs of the processive and diffusive movements are shown on the right panel

seemed plausible that KIF5C is present on vesicle populations that specifically transport cargo from the Golgi to the apical cell surface in MDCK cells.

KIF5C is present on separate immunisolated apical post-Golgi vesicle populations

The possibility that KIF5C associates with raft-carrying or raft-independent apical vesicle populations was then examined on immunisolated apical vesicles after different times of TGN release (Fig. 2c). We used MDCK_{p75-GFP} cells and MDCK cells stably expressing the raft-associated hydrolase SI, MDCK_{SI-YFP} [5]. Apical transport in MDCK_{p75-GFP} and MDCK_{SI-YFP} cells was blocked in the TGN at 20°C followed by TGN release at 37°C for various time intervals. The cells were homogenized and post-Golgi vesicles were separated by density gradient centrifugation. p75-GFP- or SI-YFP-containing vesicles were immunisolated with mAb anti-GFP antibodies and analysed by immunoblotting with KIF5A/KIF5C-specific H1 antibodies (see Table 1) for the presence of this kinesin motor. Figure 2c indicates that the H1 antibody detected a band at about 115 kDa on immunisolated p75-GFP-carrying vesicles at 5–20 min after TGN exit. The quantification revealed that the maximum value of association occurred about 10 min after TGN release followed by a moderate decline until 20 min. The possibility that this band related to the kinesin isoform KIF5A could be excluded by immunoblots with KIF5A-specific antibodies (Fig. 2c, d). Moreover, Fig. 2e depicts strong preferences of H1 antibodies for KIF5C and not for the slightly larger KIF5A on western blots from immunoprecipitates isolated from MDCK cells. In an alternative approach, vesicles were not immunoprecipitated with mAb anti-GFP, but with pAb anti-KIF5C. The presence of p75-GFP within these vesicles was then assessed by immunoblotting with mAb anti-GFP (Fig. 2c). In conjunction with our experiments depicted in the top panel, these data indicated that KIF5C-positive vesicles isolated after TGN release from p75-GFP-expressing cells carry p75-GFP. Again, the maximum intensities were detected about 5–10 min after TGN exit followed by a moderate decline, which strongly suggests that KIF5C associates with p75-containing vesicles predominantly early after TGN release.

We then determined whether KIF5C was also present on vesicles carrying raft-associated SI. Figure 2d shows that KIF5C was also present on SI-carrying vesicles. This is of great interest, since no common motor protein for both raft-associated and raft-independent pathways have yet been identified. In fact, the maximum amount of KIF5C was



found on SI-carrying vesicles isolated in an early period about 5 min after TGN release. However, in contrast to p75, the amount of KIF5C on SI vesicles decreased dramatically thereafter. This could be explained by the fact that after 5 min following TGN release the raft-associated and raft-independent routes separate and KIF5C remains more strongly associated with the raft-independent than the raft-dependent route after this separation. Again, there was no evidence for the presence of KIF5A on SI-carrying vesicles.

Thus, our observations support the model that raft-associated and raft-independent cargo is transported in an early

period after TGN release in identical transport carriers and moves along similar tracks before separation into distinct vesicle populations. As Fig. 2f depicts, there was no evidence for a direct interaction between KIF5C and the apical cargo molecules, since neither p75 nor SI coprecipitated with the kinesin motor. Galectin-3, as positive control, was successfully isolated in association with p75 as described previously [21]. This suggests, that the association between KIF5C and apical cargo is not direct and may depend on specific attachment components present on the cytosolic side of vesicular carriers that exited from the Golgi.

◀ **Fig. 2** Identification of KHC on apical post-Golgi vesicles. **a** p75-GFP carrying post-Golgi vesicles were immunoprecipitated 10 min after TGN release, separated by SDS-PAGE and immunoblotted with mAb anti-KHC (*top*), mAb anti-GFP (as a control for immunoprecipitation efficiency) and mAb anti-dynein (*bottom*). **b** Cellular homogenates of MDCK_{p75-GFP} cells were separated by density gradient centrifugation. KHC was immunoprecipitated from the vesicle-enriched fractions with H2 antibodies. The gel was stained with Coomassie (*left*) or immunoblotted with KHC antibodies (*right*). KIF5C as identified by MALDI-TOF is indicated. **c, d** For TGN accumulation of newly synthesized material, MDCK_{p75-GFP}, MDCK_{SI-YFP} and MDCK (as a control, *Ctrl*) cells were incubated at 20°C for 4 h, followed by TGN release at 37°C for specific time intervals (0, 5, 10, 15 and 20 min). Cell homogenates of MDCK_{p75-GFP} (**c**), MDCK_{SI-YFP} (**d**) and MDCK (**c, d**) cells were loaded onto a step sucrose gradient, and post-TGN vesicles were immunoprecipitated with mAb anti-GFP (**c, d**) or pAb anti-KIF5C (**c**). The immunoprecipitates were separated by SDS-PAGE and labelled with anti-KIF5A, anti-KIF5C H1 (**c, d**) or anti-GFP (**c**) antibodies by immunoblotting. Immunoblots of cell lysates are indicated as *lysate*. The *right panel* shows the quantification of band intensities relative to the total amount of protein from four independent experiments. *Asterisks* denote statistically significant differences between values from distinct time points and the maximum value using paired Student's *t* tests; **p*<0.01, ***p*<0.03. **e** Kinesin immunoprecipitation from MDCK cell lysates was performed with anti-KIF5C, anti-KIF5A and H1 antibodies. For the negative control (*neg. ctrl*) no antibody was added during immunoprecipitation. Immunoprecipitates were separated by SDS-PAGE and first immunoblotted with H1 antibodies (*top*) and thereafter, without membrane stripping, with anti-KIF5A antibodies (*bottom*). **f** p75-GFP was immunoprecipitated from MDCK_{p75-GFP} and SI-YFP from MDCK_{SI-YFP} cell lysates with anti-GFP antibodies, and KIF5C was immunoprecipitated from MDCK_{p75-GFP} and MDCK_{SI-YFP} cell lysates. The immunoprecipitates were separated by SDS-PAGE and immunoblotted with mAb H1 (anti-KIF5C), mAb anti-GFP or pAb anti-galectin-3. MDCK_{p75-GFP} cell lysate is indicated as *lysate*. For the negative control (*neg. ctrl*) no antibody was added during immunoprecipitation

Knockdown of KIF5C and KIF5B decreases the surface delivery of SI and p75

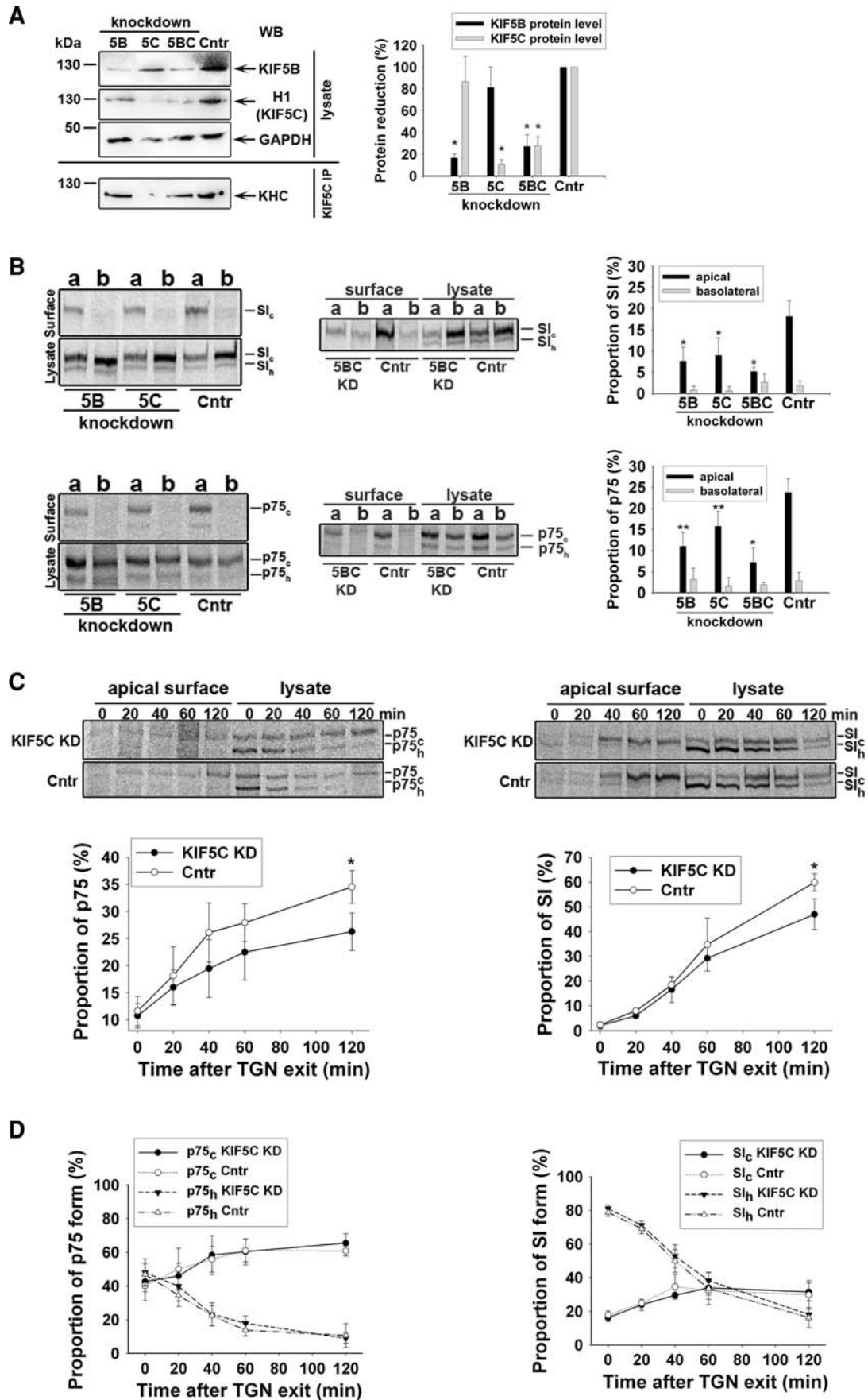
A functional role of KIF5C in apical transport was then studied by siRNA-mediated KIF5C depletion. In these experiments, KIF5B as a homologous member of the KIF5 group, which has been characterized in post-Golgi transport of p75 in epithelial cells [20], was studied for comparison. First, the specificity of knockdown for the two motor proteins was verified by immunoblotting and revealed a reduction of about 85% for each protein (Fig. 3a). To assess the consequence of this knockdown on the polarized delivery of raft-associated SI and raft-independent p75 in MDCK cells, MDCK_{SI} and MDCK_{p75} cells were biosynthetically labelled for 2 h and proteins from the apical or basolateral surface were separately immunoprecipitated. As shown in Fig. 3b, quantification revealed a significant reduction of p75 and SI at the apical membrane in KIF5B- and KIF5C-depleted cells. This indicates that both motors are involved in the intracellular transport of raft-associated SI and raft-independent p75 to the apical

cell surface and corroborates the observed influence of KIF5B on p75 trafficking in epithelial cells [20]. When KIF5B and KIF5C were knocked down in a combined approach, the remaining protein level of each kinesin was twice as high as in single knockdown cells (Fig. 3a). Nevertheless, the highest reduction in apical trafficking of the two marker proteins was achieved by this double knockdown of the two kinesins (Fig. 3b). This suggests that KIF5C is not exclusively involved in apical delivery of p75 and SI, but acts synergistically with KIF5B.

We then determined whether a trafficking delay in the absence of KIF5C was related to events following TGN exit by a transport kinetic study. Polarized cells were labelled for 15 min with [³⁵S]methionine at 37°C, rinsed with PBS and blocked for 4 h at 20°C so that all newly synthesized material accumulated in the TGN. Cells were then shifted to 37°C for different periods of time. Radioactively labelled polypeptides at the apical cell surface were then isolated by surface precipitation (Fig. 3c). In KIF5C-depleted cells the kinetics of surface delivery was significantly reduced for p75 and SI. To prove that this effect was based on a delay after TGN exit and not on a decelerated passage from ER to Golgi, the kinetics of processing from high-mannose to complex glycosylated forms of p75 and SI were quantified. As indicated in Fig. 3d, there were no significant differences in p75 or SI processing between control and KIF5C-depleted cells. Thus, a cellular role of KIF5C in trafficking of the two model proteins concentrates on the passage from the TGN to the cell surface and not on earlier steps in the secretory pathway.

KIF5C is colocalized with both p75 and SI after TGN release

Finally, we studied the intracellular localization of KIF5C in polarized MDCK cells by colocalization analysis with p75 and SI in a confocal fluorescence microscope. MDCK_{SI} cells or MDCK cells transiently transfected with p75-DsRed (MDCK_{p75-DsRed}) were immunostained for endogenous KIF5C and KIF5C-labelled intracellular vesicular structures close to the apical cell surface. Some of them were colocalized with p75-DsRed or SI (data not shown). In a more detailed analysis, the kinetics of the interactions between KIF5C and p75, SI or E-cadherin as basolateral marker were measured at various time points after TGN exit. TGN release experiments were performed as described above. As indicated in Fig. 4a,b, the two apical model proteins, p75 as well as SI, showed some overlap with KIF5C on accumulation in the TGN. Most likely, in this case a relatively high overlap coefficient of KIF5C with material accumulated in the TGN may also have been due to their condensed residence in the perinuclear area. Following TGN release, the overlap



◀ **Fig. 3** Impact of siRNA-mediated KIF5B and KIF5C depletion on apical trafficking of p75 and SI. **a** MDCK cells were grown on trans-well filters and transfected twice with KIF5B- and/or KIF5C-specific siRNA. KIF5-depleted or control cell lysates were analysed by immunoblotting with specific KIF5B and H1 (anti-KIF5C) antibodies. Anti-GAPDH antibodies were used for the loading control. To prove both KIF5C knockdown efficiency and pAb KIF5C specificity, KIF5C was immunoprecipitated from the cell lysates with the specific anti-KIF5C antibodies. The immunoprecipitates were separated by SDS-PAGE and immunoblotted with KHC antibodies (*bottom of left panel*). In the *right panel* quantifications of four independent experiments are shown. **b** MDCK_{p75-GFP} and MDCK_{SI} cells were grown on trans-well filters and biosynthetically labelled with [³⁵S]methionine for 2 h in the presence of KIF5 isotype-specific siRNA or luciferase siRNA for control. Cell surface immunoprecipitation of p75 and SI from the apical (*a*) and basolateral (*b*) surfaces was performed with the corresponding antibodies, and cytosolic p75 and SI were precipitated from the remaining cell lysates for comparison. The immunoprecipitates were subjected to SDS-PAGE followed by phosphorimaging. The *left panel* shows representative gels of individual KIF5 knockdown experiments. The proportions of SI and p75 from three independent experiments were quantified (*right panel*). **c** Control or KIF5C knockdown MDCK_{p75-GFP} and MDCK_{SI} cells were grown on trans-well filters and biosynthetically labelled with [³⁵S]methionine for 15 min. The cells were incubated at 20°C for 4 h to block newly synthesized proteins in the TGN. The cells were then shifted to 37°C for various time intervals, followed by cell surface immunoprecipitation of p75 and SI from the apical surface. Cytosolic p75 and SI were immunoprecipitated from the remaining cell lysates for comparison. The immunoprecipitates were subjected to SDS-PAGE, followed by phosphorimaging. High mannose (p75_h and SI_h) or complex glycosylated (p75_c and SI_c) forms are indicated. The proportions of surface p75 and SI were quantified from four independent experiments. **d** The kinetics of processing from high-mannose to complex glycosylated forms of p75 and SI in control and KIF5C-depleted cells as shown in **c** were quantified. *Asterisks* denote statistically significant differences using paired Student's *t* tests; **p*<0.01, ***p*<0.03

coefficient reached a maximum after 5 min and dropped to a minimum after 20 min. Interestingly, the kinetics for both p75 and SI were quite similar. On the other hand, the overlap coefficient of KIF5C with basolateral E-cadherin dropped to a minimum directly after TGN exit (see supplementary material Fig. 1), which suggests that KIF5C is not involved in post-Golgi basolateral trafficking of epithelial cells. These experiments demonstrate that post-Golgi transport carriers for raft-dependent and raft-independent apical cargo are at first decorated by the kinesin motor KIF5C followed by a switch to other motor proteins thereafter.

We then determined by fluorescence microscopy whether KIF5C depletion altered the cellular trafficking of p75 and SI. Since KIF5C expression was transiently depleted, the specific knockdown was visible in some unevenly distributed cells of a polarized epithelium, while other cells still expressed normal levels of the motor. Figure 4c shows that p75-DsRed and SI accumulated in relatively large vesicles of KIF5C-depleted cells, suggesting that their transport was blocked intracellularly. On the other hand, the distribution of p75 and SI in KIF5C-expressing cells

was normal. These observations corroborate our biochemical data enabling us to conclude that KIF5C plays a functional role in the early steps of post-Golgi trafficking of apical transmembrane proteins comprising raft-associated and raft-independent cargo.

Discussion

In this study we demonstrated that KIF5C is a novel motor protein involved in apical protein transport of polarized MDCK cells. Evidence for the presence of a microtubular motor on isolated apical vesicles came from *in vitro* motility assays, where we recorded unidirectional movements with velocities of about 0.28 μm/s. This is consistent with recently published data on the diffusive and processive movement of kinesin-1 motors [25]. In general, the velocities of conventional kinesins may vary depending on the study approach. For gliding assays the pace of KIF1B was about 0.66 μm/s [26], whereas beads were transported in motility assays by the same kinesin with a velocity up to 0.82 μm/s [27]. Moreover, KIF5B-dependent movement of apical cargo in living cells was about 1.4 μm/s [20]. A plausible reason for this variability may be the presence of cofactors that substantially influence kinesin velocity and thus vesicle movement [28].

KIF5C was then identified on apical transport vesicles by mass spectrometry and immunodetection. This kinesin occurs in conjunction with KIF5B and KIF5A a member of the KIF5 group. At first, KIF5C was thought to be expressed exclusively in neurons, preferentially in motor neurons. In the absence of this motor, KIF5C knockdown mice have a smaller brain, but are viable with a relative loss of motor neurons to sensory neurons [29]. Moreover, KIF5C also plays a role in morphogenetic processes, as shown in chicken embryos [30]. Here, the KIF5C expression during embryo development is not restricted to neuroectoderm-derived structures, but is additionally found in epithelial somites. Furthermore, Jaulin et al. [20] detected KIF5C in epithelial A549 and MCF-7 cells. The concrete function of KIF5C in non-neuronal tissues, however, has not yet been described. In neurons this motor plays a role in anterograde trafficking of mitochondria and vesicles [31]. KIF5C binds its cargo at the C-terminus of KHC or by association with two kinesin light chains. This interaction is mediated by the adaptor protein GRIP1, which forms a ternary complex with the two KIF5C heavy and light chains [31]. GRIP1 also forms a complex with GluR2, a subunit of the AMPA (α-amino-3-hydroxy-5-methylisoxazole-4-propionate) receptor [32], and thus KIF5C is linked to synaptic vesicle components in neuronal cells. In view of the fact that our data did not reveal a permanent linkage between apical cargo and KIF5C in

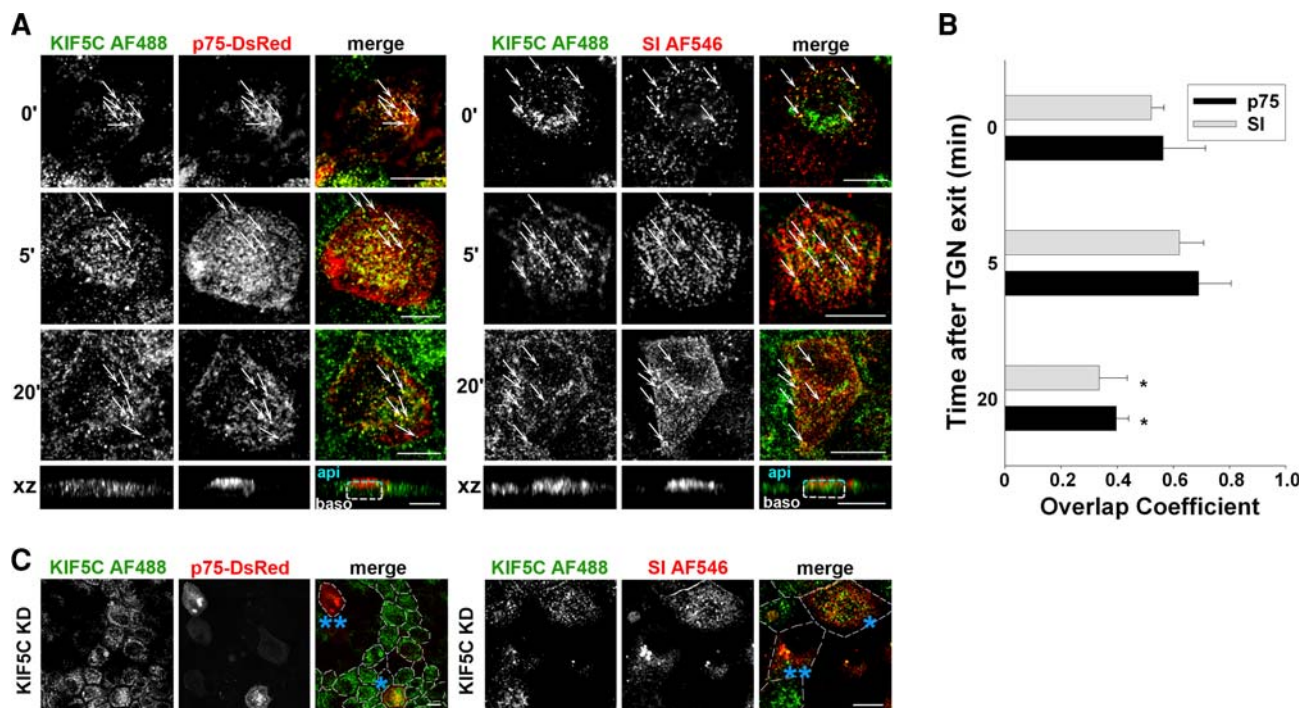


Fig. 4 Confocal fluorescence microscopic analysis of KIF5C colocalization with p75 and SI in MDCK cells. **a** MDCK cells transiently transfected with p75-DsRed or the stable MDCK cell line expressing SI (MDCK_{SI}) were used. The cells were blocked for 4 h at 20°C so that newly synthesized proteins accumulated in the TGN. After TGN release at 37°C for 0, 5 and 20 min, cells were fixed and stained for endogenous KIF5C (with Alexa Fluor 488 as secondary antibody) and SI (with Alexa Fluor 546 as secondary antibody). Confocal microscopic sections were recorded from regions just beneath the apical membrane. *Arrows* colocalized structures; *bottom row xz* views; *api* apical region, *baso* basolateral region. **b** Overlap coefficients between KIF5C and p75 or SI fluorescence were quantified from 20 cells for

each time point after TGN release. *Asterisks* denote statistically significant differences between time points 5 and 20 min using paired Student's *t* tests; $*p < 0.001$. **c** MDCK cells stably expressing SI or transiently transfected with p75-DsRed were transfected twice with KIF5C-specific siRNA. On the fifth day after seeding the cells were fixed and stained specifically for endogenous KIF5C (with secondary Alexa Fluor 488 antibodies). Images were taken from the apical area and *dashed lines* roughly indicate cell borders. The cells with high levels of KIF5C expression are indicated by *one blue asterisk*, and the KIF5C-depleted cells by *two blue asterisks*. In the merged images KIF5C is shown in *green*, and p75 and SI in *red*. *Scale bars* 10 μ m

epithelial cells, this interaction could be only transient or mediated by alternative vesicle-associated binding partners. Evidence for the specific targeting of KIF5C to distinct cellular sites comes from experiments that have demonstrated a preferential binding and trafficking of KIF5C along detyrosinated microtubules [33]. Tubulin tyrosination can discriminate axonal microtubules from somatodendritic microtubules, and thus specifically recruit kinesin-1 motors to axonal or somatodendritic microtubules in polarized neurons [34]. However, in MDCK cells the distribution of this particular microtubular subtype is not yet clear.

Another important question deals with the concrete subcellular trafficking routes and compartments that are interconnected by KIF5C-mediated transport. At least for some apical transmembrane proteins, trafficking from the TGN to the plasma membrane of MDCK cells encompasses the passage through endosomal compartments before raft-dependent and raft-independent routes separate [22, 35]. Based on the observation that this transendosomal passage

proceeds during a time period of about 10 min after TGN release, a maximal association between KIF5C and p75- and SI-containing carriers in this period suggests that KIF5C is mainly responsible for these early steps in apical post-Golgi trafficking. Supporting evidence for a general role of KIF5 family members in endosomal post-Golgi trafficking comes from a recent study on the regulation of endosomal transport by a gadkin/AP-1/KIF5-complex [36]. Although we were able to exclude the presence of KIF5A on apical carriers, KIF5C is not the only KIF5 isotype involved in apical trafficking, since KIF5B is also required for this cellular process [20]. This view is supported by knockdown experiments performed in our study and by the finding of relatively mild phenotypes in KIF5C knockout mice [29]. Thus, a lack of KIF5C in intracellular trafficking events could be compensated for by alternative motor proteins. In addition, our data suggest that KIF5C as well as the isotype KIF5B are both involved in the surface delivery of raft-associated and raft-independent apical glycoproteins. Depletion of only one of them affects apical transport

efficiency. This effect can be enhanced by double knock-down of both kinesins, which indicates that KIF5B and KIF5C act in concert and have equivalent functions in apical protein trafficking. The idea, that more than one kinesin motor transports apical cargo molecules following TGN exit is supported by the identification so far of three kinesins in apical trafficking of MDCK cells: KIFC3 [19], KIF5B [20] and KIF5C. An involvement of a subset of microtubular motors in a specific pathway to the cell surface implies that the motor activities themselves as well as the pool of transported cargo are strictly adjusted by cellular control mechanisms. These mechanisms have not yet been elucidated and participating regulatory elements will have to be identified in future studies.

Our results suggest that a relatively new member of the KIF5 kinesin motors, KIF5C, is required for early post-Golgi trafficking of raft-associated and raft-independent apical glycoproteins, most likely in common vesicles, and delivers its cargo through endosomal compartments beneath the apical cell surface.

Acknowledgment We are grateful to M. Dienst for technical assistance. Antibodies against SI and p75 were generous gifts from H.P. Hauri (Biocenter, University of Basel, Switzerland) and A. Le Bivic (Faculté des Sciences de Luminy, Marseille, France). This work was supported by the Deutsche Forschungsgemeinschaft (DFG), Bonn, Germany (grants JA 1033, Graduiertenkolleg 1216 and Sonderforschungsbereich 593).

References

- Rodriguez-Boulan E, Powell SK (1992) Polarity of epithelial and neuronal cells. *Annu Rev Cell Biol* 8:395–427
- Danielsen EM, Hansen GH (2008) Lipid raft organization and function in the small intestinal brush border. *J Physiol Biochem* 64:377–382
- Delacour D, Jacob R (2006) Apical protein transport. *Cell Mol Life Sci* 63:2491–2505
- Griffiths G, Simons K (1986) The trans Golgi network: sorting at the exit site of the Golgi complex. *Science* 234:438–443
- Jacob R, Naim HY (2001) Apical membrane proteins are transported in distinct vesicular carriers. *Curr Biol* 11:1444–1450
- Jacob R, Heine M, Alfalah M, Naim HY (2003) Distinct cytoskeletal tracks direct individual vesicle populations to the apical membrane of epithelial cells. *Curr Biol* 13:607–612
- Danielsen EM (1995) Involvement of detergent-insoluble complexes in the intracellular transport of intestinal brush border enzymes. *Biochemistry* 34:1596–1605
- Fiedler K, Kobayashi T, Kurzchalia TV, Simons K (1993) Glycosphingolipid-enriched, detergent-insoluble complexes in protein sorting in epithelial cells. *Biochemistry* 32:6365–6373
- Ojakian GK, Schwimmer R (1988) The polarized distribution of an apical cell surface glycoprotein is maintained by interactions with the cytoskeleton of Madin-Darby canine kidney cells. *J Cell Biol* 107:2377–2387
- Zurzolo C, van't Hof W, van Meer G, Rodriguez-Boulan E (1994) VIP21/caveolin, glycosphingolipid clusters and the sorting of glycosylphosphatidylinositol-anchored proteins in epithelial cells. *EMBO J* 13:42–53
- Yeaman C, Le Gall AH, Baldwin AN, Monlauzeur L, Le Bivic A, Rodriguez-Boulan E (1997) The O-glycosylated stalk domain is required for apical sorting of neurotrophin receptors in polarized MDCK cells. *J Cell Biol* 139:929–940
- Le Bivic A, Sambuy Y, Mostov K, Rodriguez-Boulan E (1990) Vectorial targeting of an endogenous apical membrane sialoglycoprotein and ovomorulin in MDCK cells. *J Cell Biol* 110:1533–1539
- Verkade P, Harder T, Lafont F, Simons K (2000) Induction of caveolae in the apical plasma membrane of Madin-Darby canine kidney cells. *J Cell Biol* 148:727–739
- Ihrke G, Bruns JR, Luzio JP, Weisz OA (2001) Competing sorting signals guide endolyn along a novel route to lysosomes in MDCK cells. *EMBO J* 20:6256–6264
- Jacob R, Alfalah M, Grunberg J, Obendorf M, Naim HY (2000) Structural determinants required for apical sorting of an intestinal brush-border membrane protein. *J Biol Chem* 275:6566–6572
- Musch A (2004) Microtubule organization and function in epithelial cells. *Traffic* 5:1–9
- Bacallao R, Antony C, Dotti C, Karsenti E, Stelzer EH, Simons K (1989) The subcellular organization of Madin-Darby canine kidney cells during the formation of a polarized epithelium. *J Cell Biol* 109:2817–2832
- Lafont F, Burkhardt JK, Simons K (1994) Involvement of microtubule motors in basolateral and apical transport in kidney cells. *Nature* 372:801–803
- Noda Y, Okada Y, Saito N, Setou M, Xu Y, Zhang Z, Hirokawa N (2001) KIFC3, a microtubule minus end-directed motor for the apical transport of annexin XIIIb-associated Triton-insoluble membranes. *J Cell Biol* 155:77–88
- Jaulin F, Xue X, Rodriguez-Boulan E, Kreitzer G (2007) Polarization-dependent selective transport to the apical membrane by KIF5B in MDCK cells. *Dev Cell* 13:511–522
- Delacour D, Cramm-Behrens CI, Drobecq H, Le Bivic A, Naim HY, Jacob R (2006) Requirement for galectin-3 in apical protein sorting. *Curr Biol* 16:408–414
- Cramm-Behrens CI, Dienst M, Jacob R (2008) Apical cargo traverses endosomal compartments on the passage to the cell surface. *Traffic* 9:2206–2220
- Murray JW, Bananis E, Wolkoff AW (2000) Reconstitution of ATP-dependent movement of endocytic vesicles along microtubules in vitro: an oscillatory bidirectional process. *Mol Biol Cell* 11:419–433
- Blocker A, Severin FF, Habermann A, Hyman AA, Griffiths G, Burkhardt JK (1996) Microtubule-associated protein-dependent binding of phagosomes to microtubules. *J Biol Chem* 271:3803–3811
- Lu H, Ali MY, Bookwalter CS, Warshaw DM, Trybus KM (2009) Diffusive movement of processive kinesin-1 on microtubules. *Traffic* 10:1429–1438
- Nangaku M, Sato-Yoshitake R, Okada Y, Noda Y, Takemura R, Yamazaki H, Hirokawa N (1994) KIF1B, a novel microtubule plus end-directed monomeric motor protein for transport of mitochondria. *Cell* 79:1209–1220
- Wozniak MJ, Melzer M, Dorner C, Haring HU, Lammers R (2005) The novel protein KBP regulates mitochondria localization by interaction with a kinesin-like protein. *BMC Cell Biol* 6:35
- Bohm KJ, Stracke R, Unger E (2000) Speeding up kinesin-driven microtubule gliding in vitro by variation of cofactor composition and physicochemical parameters. *Cell Biol Int* 24:335–341
- Kanai Y, Okada Y, Tanaka Y, Harada A, Terada S, Hirokawa N (2000) KIF5C, a novel neuronal kinesin enriched in motor neurons. *J Neurosci* 20:6374–6384
- Dathe V, Pröls F, Brand-Saberi B (2004) Expression of kinesin kif5c during chick development. *Anat Embryol (Berl)* 207:475–480

31. Smith MJ, Pozo K, Brickley K, Stephenson FA (2006) Mapping the GRIF-1 binding domain of the kinesin, KIF5C, substantiates a role for GRIF-1 as an adaptor protein in the anterograde trafficking of cargoes. *J Biol Chem* 281:27216–27228
32. Setou M, Seog DH, Tanaka Y, Kanai Y, Takei Y, Kawagishi M, Hirokawa N (2002) Glutamate-receptor-interacting protein GRIP1 directly steers kinesin to dendrites. *Nature* 417:83–87
33. Dunn S, Morrison EE, Liverpool TB, Molina-Paris C, Cross RA, Alonso MC, Peckham M (2008) Differential trafficking of Kif5c on tyrosinated and detyrosinated microtubules in live cells. *J Cell Sci* 121:1085–1095
34. Konishi Y, Setou M (2009) Tubulin tyrosination navigates the kinesin-1 motor domain to axons. *Nat Neurosci* 12:559–567
35. Cresawn KO, Potter BA, Oztan A, Guerriero CJ, Ihrke G, Goldenring JR, Apodaca G, Weisz OA (2007) Differential involvement of endocytic compartments in the biosynthetic traffic of apical proteins. *EMBO J* 26:3737–3748
36. Schmidt MR, Maritzen T, Kukhtina V, Higman VA, Doglio L, Barak NN, Strauss H, Oschkinat H, Dotti CG, Haucke V (2009) Regulation of endosomal membrane traffic by a Gadkin/AP-1/ kinesin KIF5 complex. *Proc Natl Acad Sci U S A* 106:15344–15349
37. Cai Y, Singh BB, Aslanukov A, Zhao H, Ferreira PA (2001) The docking of kinesins, KIF5B and KIF5C, to Ran-binding protein 2 (RanBP2) is mediated via a novel RanBP2 domain. *J Biol Chem* 276:41594–41602